Biuletyn WAT
Vol. LXVII, Nr 2, 2018

# The impact of the magnetization direction on the static and dynamic parameters of an electromagnetic linear actuator

KRZYSZTOF JUST[1], PAWEŁ PISKUR[2]

[1]1st Airlift Base, 1c Żwirki i Wigury Str., 00-909 Warsaw, Poland, justk5@op.pl
[2]Polish Naval Academy, Faculty of Mechanical and Electrical Engineering, Department of Marine Electrical and Automation Engineering, Laboratory of Marine Automation Engineering, 69 J. Śmidowicza Str., 81-127 Gdynia, Poland, p.piskur@amw.gdynia.pl

**Abstract.** This paper presents a simulation analysis of the impact of magnetization direction on the static and dynamic parameters of an electromagnetic linear actuator. The simulation analysis computations were completed for three different magnetization configurations of permanent magnets (i.e. axial, radial, and a Halbach array). The finite element method (FEM) was applied which provided a good representation of the properties of actual physical objects. The computations enabled an investigation into and an assessment of the impact of the runner magnetization method on the static and dynamic properties of the drive.
**Keywords:** modelling and simulation, electromagnetic actuator, finite element method, field analysis, Halbach array
**DOI:** 10.5604/01.3001.0012.0956

## 1. Introduction

The design engineering of electromechanical drives is focused on providing the best performance parameters achievable (a high speed of movement and a high thrust force) at the simplest structure of the drive system and a minimum consumption of fabrication materials. Both objectives can be achieved with suitable drive control systems or suitable design solutions.

The requirements to be met by a linear actuator (i.e. a high thrust force, a specific runner travel, high rigidity, low mass, and thermal stability) are often in conflict with

one another; a compromise needed to achieve all the specified requirements is often problematic due to design and material considerations. The thrust force generated by a drive unit depends on the magnetic induction value at which the magnetic core is at its saturation point. The saturation induction value depends on the type and properties of the material which the magnetic circuit is made from.

The magnetic field distribution in permanent magnet devices depends both on the anisotropy (the thermomagnetic processing) of permanent magnets and the direction of their magnetization (which can be axial, radial, or a Halbach array). If the air gap is kept uniform, two types of magnetic field distribution can be obtained: trapezoid or near-sinusoidal. The correct direction of the magnetic field in the air gap improves the static and dynamic properties of permanent magnet drive units.

All relations between the decisive parameters which characterize the properties of a drive unit can be determined with analytical computations. However, analytical computations are biased by numerous errors caused by the imprecision of the analytical model and the assumptions made for simplification. Hence, analytical calculations have been increasingly replaced with FEM (finite element method) computations. The application of FEM enables precise and reliable simulation computations; FEM allows inclusion of most physical phenomena which occur in real-life objects.

This paper presents an analysis of the effects of the direction of magnetization of permanent magnets on the static characteristics (magnetic field distribution, electromagnetic force (cogging of and thrust)) and dynamic characteristics (displacement, velocity and force in time) of an electromagnetic drive unit in Comsol Multiphysics, a FEM-based computational environment.

## 2. Description of the model of the electromagnetic linear actuator

The test object of this work was a single-segment electromagnetic linear actuator which featured permanent magnets and a cylindrical design (Fig. 1); the test object was selected due to its advantages: a simple design, ease of control, high acceleration, and low fabrication costs. The electromagnetic linear actuator comprised an immobile coil in a ferromagnetic casing, and a runner, comprising annular permanent magnets connected to ferromagnetic rings.

The first stage of this work was an analysis of the magnetic field generated by the permanent magnets (within the area of the runner); hence, the field generated by the current flow through the coil was not considered. Three runner topologies, each with a different direction of the magnetization vector, were investigated (Fig. 2). The computations included neodymium magnets (NdFeB) with a remanence induction $B_r = 1.23$ [T] an energy density 400 kJ/m$^3$.

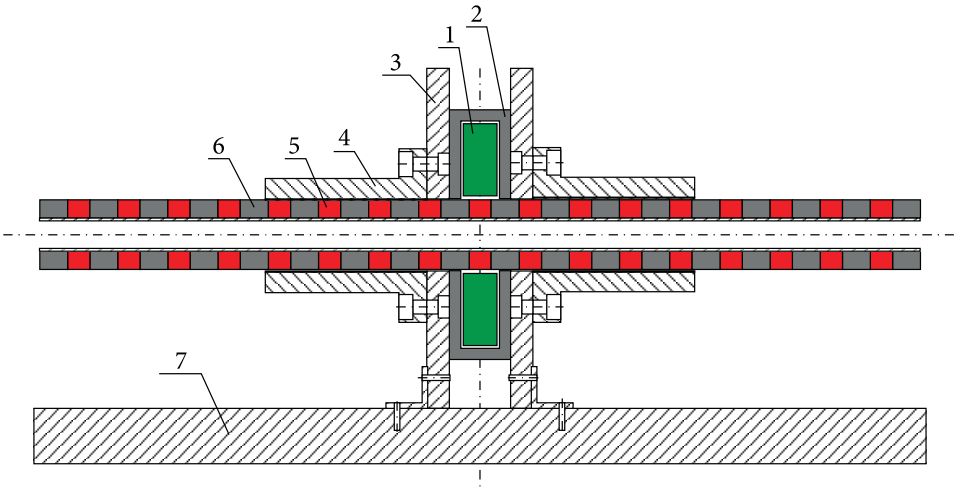


Fig. 1. Diagram of the electromagnetic linear actuator: 1 — coil; 2 — ferromagnetic casing; 3 — aluminium shield; 4 — linear bearing; 5 — permanent magnet; 6 — ferromagnetic ring; 7 — base

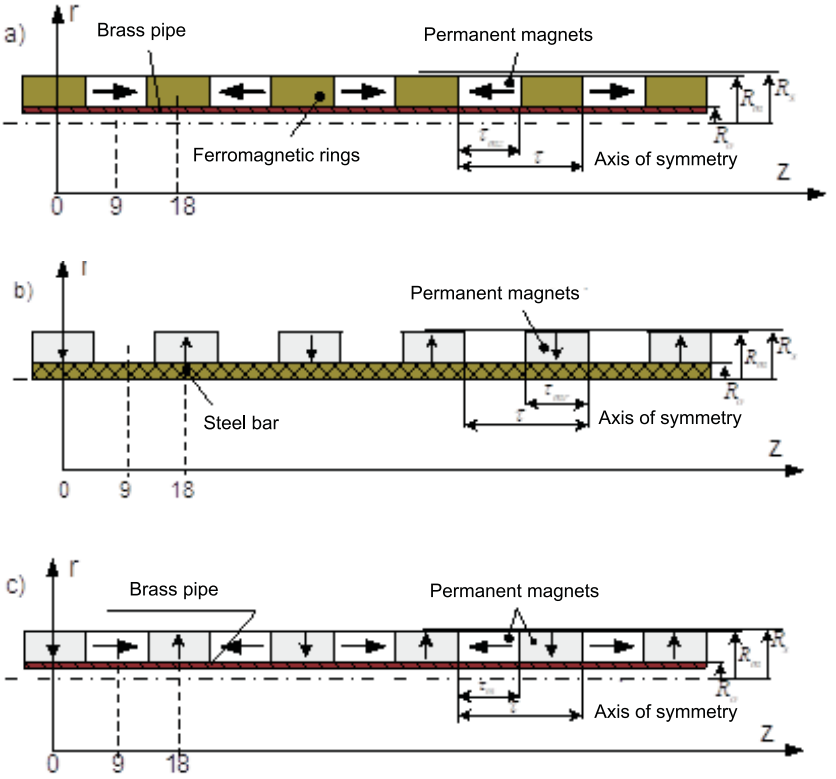


Fig. 2. Runner magnetization configurations: (a) axial; (b) radial; (c) Halbach array

The radial dimensions of the computational models are, respectively: $R_0$; $R_m$ — inner radius and outer radius; $R_s = R_m + g$ — runner outer radius; $g$ — air gap size; $h_m$ — permanent magnet thickness; $\tau_m = \tau_{mr} = \tau_m$ — permanent magnet width; $\tau_m$ — runner pole pitch.

The configurations of the permanent magnets (Fig. 2) forced different structural solutions of the runner of the electromagnetic linear actuator. For the radial configuration, the runner was made as a ferromagnetic bar on which radially magnetized permanent magnets were placed (Fig. 2b). The runner was a carrier component which provided mechanical symmetry and a suitable direction of the magnetic field. For the axial configuration (Fig. 2a), the runner was built from permanent magnets joined with ferromagnetic rings, and the runner components were placed on a brass tube to provide mechanical symmetry of the system. The discrete Halbach array (Fig. 2c) was built with annular permanent magnets with axial and radial directions of magnetization and arranged alternately on a brass tube in a suitable configuration.

Fig. 3 shows section AB, parallel to the runner axis and offset by 1 mm from the runner (where the offset was the air gap). The radial and axial components of magnetic induction were evaluated along section AB.

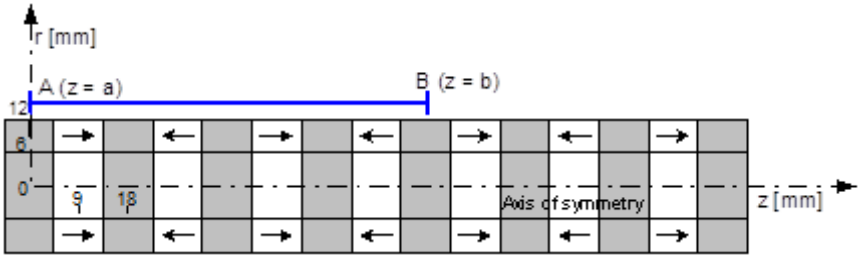


Fig. 3. Measurement section AB (a = 0, b = 72 mm) offset 1 mm from the runner surface

## 3. Computations of the effect of the magnetization direction of the runner on the static characteristics of the actuator

The static characteristics included the distributions of magnetic induction in the air gap and the characteristics of electromagnetic force as a function of displacement. They formed the foundation for a polar circumferential computational model applied in the testing of the dynamic properties of the actuator. The analysis included testing of the magnetic field distribution in the air gap (the axial and radial magnetic induction components) and the effect of the magnetization vector direction of the permanent magnets on the generated magnetic force (of cogging and thrust). The results of the analysis are shown in the charts below.

The distribution of the axial magnetic induction component (Fig. 4) was approximate to trapezoid distribution. In the axial and Halbach array configurations, the axial magnetic induction component had the maximum values directly over the surface of the permanent magnets; the values dropped rapidly outside the area directly at the permanent magnets and reached zero in the middle of height of each ferromagnetic ring (for the axial magnetization) or of the radially magnetized permanent magnet (for the Halbach array). In the radial configuration, the axial magnetic induction component reached zero exactly in the middle of the permanent magnets; it reached the highest values within the air gap part between the permanent magnets.

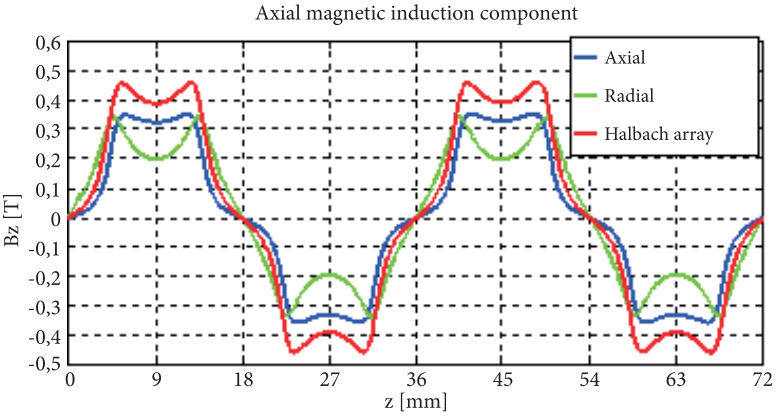


Fig. 4. Chart of the axial magnetic induction component in different permanent magnet configurations

The distribution of the radial magnetic induction component (Fig. 5) was different than for the axial component and resulted from the ferromagnetic components in the structure of the runner. In the axial and Halbach array configurations, the radial magnetic induction component had the maximum values at the centres of the ferromagnetic rings (for the axial magnetization) and the centres of the radially magnetized permanent magnets (for the Halbach array), and reached zero at the centres of the axially magnetized permanent magnets. In the radial configuration, the distribution of the radial magnetic induction component was nearly sinusoidal. The maximum values were directly over the surface of the permanent magnets; the radial magnetic induction component dropped outside the surface and reached zero in the middle of the distance between the permanent magnets (within the air gap).

The direction of the magnetization vector of the permanent magnets had a significant effect on the determined static characteristics. The computations were completed for two states of power supply: zero current and the maximum current

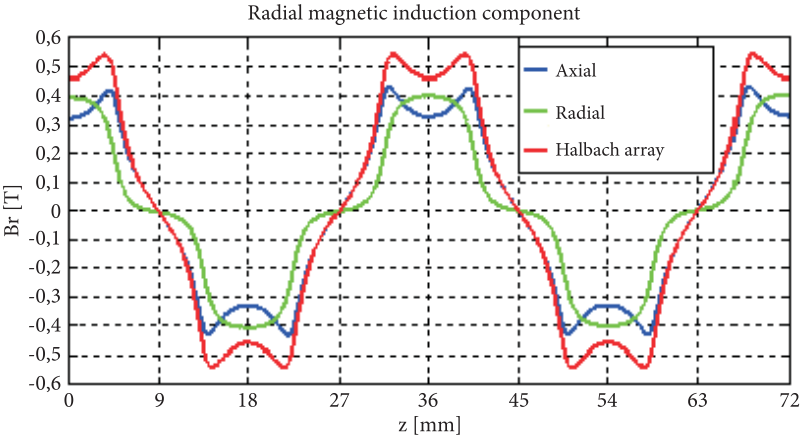


Fig. 5. Chart of the radial magnetic induction component in different permanent magnet configurations

(at 8 A) flowing through the coil windings. The cogging force of the permanent magnets (Fig. 6) (in the zero current state) reached zero at the neutral positions of the runner; this configuration repeated every half of the pole pitch. Proper formation of the magnetic field in the air gap had an essential effect on the cogging force; the maximum and minimum values which were achieved for the Halbach array configuration (48 N) and, respectively, for the radial magnetization configuration (20 N). The radial magnetization affected the value of the thrust force (at the maximum current supply state of the coil windings) with was 50% less than in other magnetization configurations (100 N). The results obtained for the axial magnetization and Halbach array configurations (Fig. 7) were approximate and differed only by several percent (i.e. 175 N).

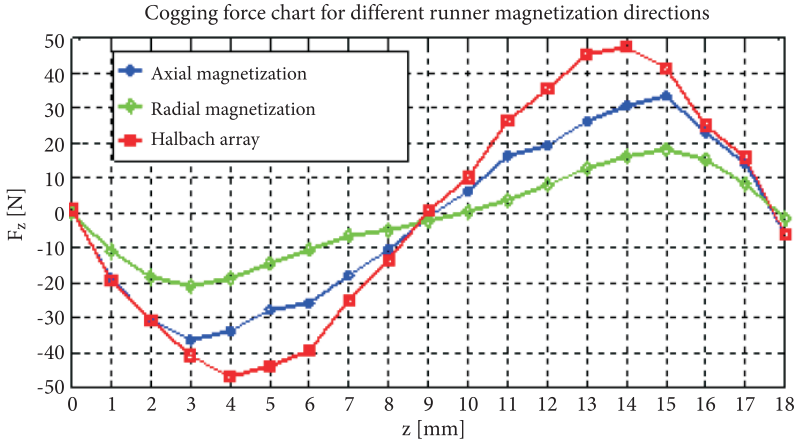


Fig. 6. Chart of cogging force vs. runner position

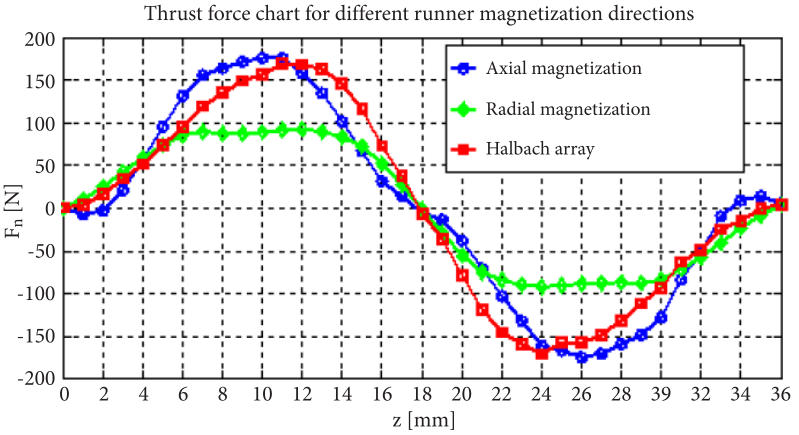


Fig. 7. Chart of thrust force vs. runner position

## 4. Computations of the effect of the magnetization direction of the runner on the dynamic characteristics of the actuator

The simulation model of the electromagnetic linear actuator was built in an FEM (finite element method) environment, Comsol Multiphysics. This FEM environment was chosen due its high versatility and availability. Comsol Multiphysics allowed for the testing of static and dynamic phenomena in electromagnetic fields and simulating displacement of components tested. The field model facilitated an accurate representation of the real-life object in the analysis and the verification of the mathematical model without building a physical prototype.

The computations included the axial symmetry of the electromagnetic linear actuator (i.e. axially symmetrical models were applied). The coil windings of the electromagnetic linear actuator were powered with a square direct current pulse at an amplitude of 20 V; the output was the current flowing through the coil, the displacement, and the magnetic force. A discrete change of voltage caused an exponential increase of the current; the related curve slope depended on the time constant of the circuit (L/R). Propelled by the direct current pulse, the runner moved (Fig. 8) by one half of the pole pitch, i.e. 18 mm. The shortest stabilization time of the runner in the neutral position was in the radial magnetization configuration. The Halbach array extended the stabilization time to 0.225 s.

The maximum velocities of motion (Fig. 9) in the axial and Halbach array magnetization configurations were approximate; however, in the axial magnetization configuration, the runner decelerated faster inside the coil supplied with power. In the radial magnetization configuration, the motion velocity was lower and at 0.75 m/s.

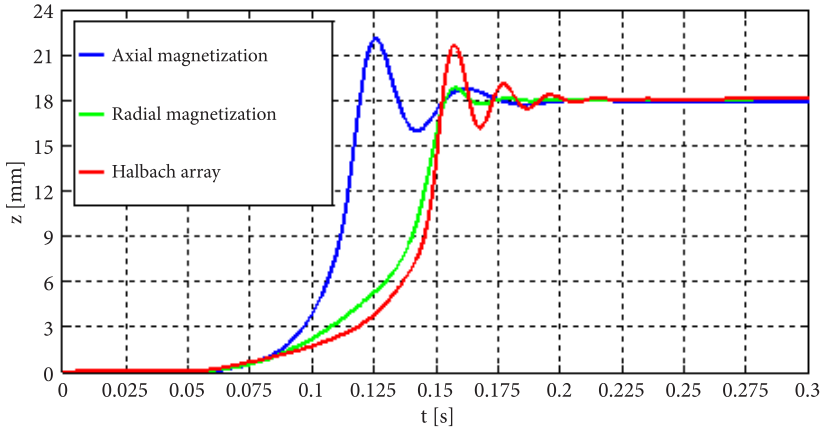


Fig. 8. Chart of runner displacement vs. time for various magnetization directions

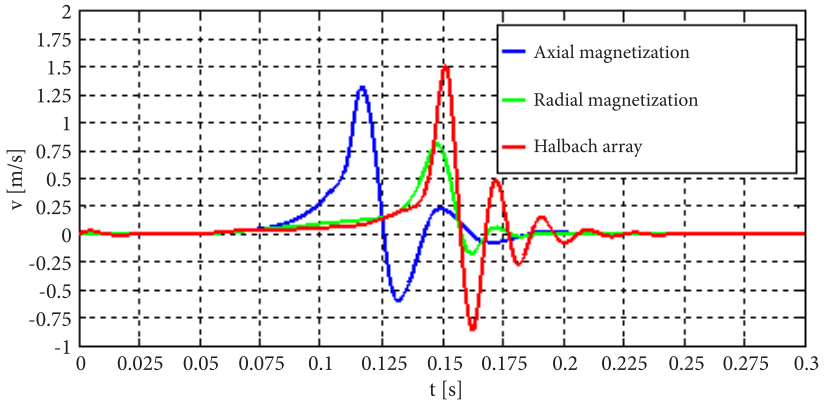


Fig. 9. Chart of runner velocity vs. time for various magnetization directions

The electromagnetic force did not reach a steady value until the transient state passed. In the radial configuration of the permanent magnets, the electromagnetic force was 30% lower than in the axial and Halbach array configurations (Fig. 10).

The analysis proved that the best dynamic properties of the electromagnetic actuator could be achieved in the radial or axial magnetization configuration (where the highest magnetic flux values were present with high forces and a suitable runner stabilization time). Given the difficulty with the manufacturing of radially magnetized permanent magnets, resulting in high market prices of the products, and the high availability of the permanent magnets with the radial magnetizing direction, it would be cost-effective to choose the axial magnetization direction for the runner.

Fig. 11 illustrates the magnetic field distribution in the electromagnetic linear actuator with the axial magnetization of the runner, the coil powered at 8 A, and two different positions of the runner. The magnetic field generated by the flow of current

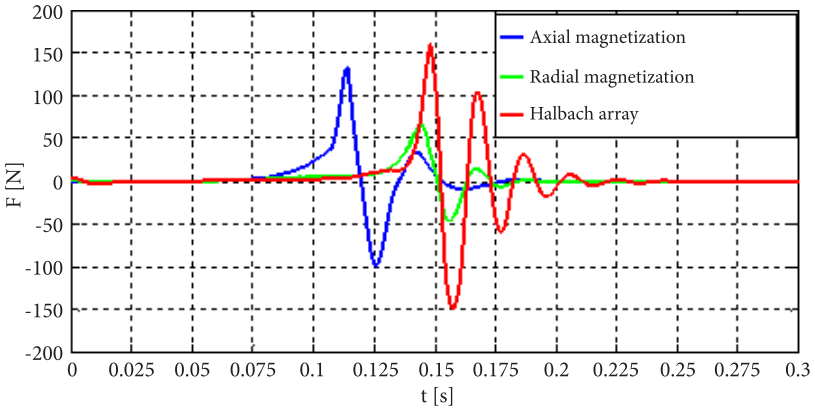


Fig. 10. Chart of the magnetic force vs. time for various magnetization directions

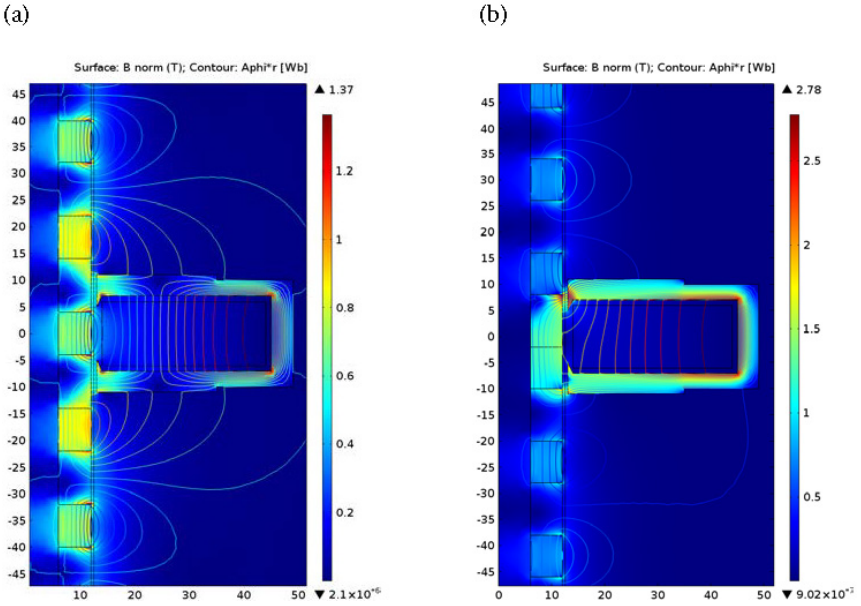


Fig. 11. Magnetic field distribution in the single-coil electromagnetic linear actuator powered at 8 A and with the following runner positions relative to the solenoid centre: (a) 0 mm; (b) 12 mm

countered the field of the permanent magnet and naturally repulsed it. Both magnetic fields mitigate themselves. In the specific positions of the runner (Fig. 11), the most saturated components were the ferromagnetic casing parts and the runner parts near the air gap. The force field lines were focused within the ferromagnetic ring between the magnets with opposing directions of magnetization. At the displacement of 12 mm, the amplified magnetization of both fluxes nearly saturated the magnetic material (with the induction value significantly above 2 T). In other subareas, the magnetic induction was lower and did not exceed 1.5 T.

## 5. Conclusion

The work presented in this paper included a simulation analysis of the impact of magnetization direction on the static and dynamic properties of an electromagnetic linear actuator. The analysis included an estimation of the magnetic field distribution (the magnetic induction components within the runner), the directions of magnetic force (of cogging and thrust) in the function of the magnet position relative to the centre of the coil, and the testing of dynamic properties of the electromagnetic linear drive, which itself included plotting of displacement, velocity and force, each versus time.

The maximum magnetic flux densities were obtained for the Halbach array magnetization configuration. The minimum magnetic flux densities were obtained for the radial magnetization configuration. The dynamic testing of the electromagnetic linear actuator demonstrated that its best dynamic properties could be achieved in the axial and Halbach array magnetization configurations, resulting in high acceleration and force values. The application of the axial magnetization configuration in the runner had a shorter stabilization time of the runner in its neutral position than in the Halbach array magnetization configuration.

This work was funded personally by the authors.

*Received February 20, 2018. Revised April 6, 2018.*

Paper translated into English and verified by company SKRIVANEK sp. z o.o., 22 Solec Street, 00-410 Warsaw, Poland.

REFERENCES

[1] COMSOL Multiphysics: *AC/DC Module User's Guide.*

[2] Gieras J.F., *Linear induction drives*, Clarendom Press, Oxford, 1994.

[3] Gierak D., Dudzikowski I., *Analiza Wpływu Sposobu Namagnesowania Magnesów na Parametry Silnika Komutatorowego o Magnesach Trwałych*, Prace Naukowe Instytutu Maszyn, Napędów i Pomiarów Elektrycznych Politechniki Wrocławskiej, nr 60, Wrocław, 2007.

[4] Henzel M., Falkowski K., Żokowski M., The *analysis of the control system for the bearingless induction electric motor, Journal of Vibroengineering*, vol. 14, issue 1, March 2012, pp. 16-21.

[5] Humphries S., *Finite-element Methods for Electromagnetics*, Field Precision LLC, 2010.

[6] Just K., Piskur P., Bielawski R., *Experimental verification of the one-phase linear actuator with permanent magnets for robotic system applications*, Measurement Automation Monitoring, 2018 (in publishing).

[7] Just K., Tarnowski W., *Field model of electromechanical phenomena in the linear drive with permanent magnets*, Biuletyn WAT, vol. 66, nr 3, 2017.

[8] Just K., *Metodyka projektowania konstrukcji i sterowania mechatronicznego urządzenia wykonawczego ruchu liniowego,* rozprawa doktorska, Wydział Technologii i Edukacji Politechniki Koszalińskiej, Koszalin, 2018.

[9] Seok-Myeong Jang, Jang-Young Choi, Sung-Ho Lee, Han-Wook Cho, Won-Bum Jang, *Analysis and Experimental Verification of Moving-Magnet Linear Actuator with Cylindrical Halbach Array*, IEEE Transactions on Magnetics, vol. 40, no. 4, July 2004.

[10] Seok-Myeong Jang, Jang-Young Choi, Han-Wook Cho, Sung-Ho Lee, *Analysis and Control Parameter Estimation of a Tubular Linear Motor with Halbach and Radial Magnet Array*, KIEE International Transactions on Electrical Machinery and Energy Conversion Systems, vol. 5-B, no. 2, 2005, pp. 154-161.

[11] Piskur P., Tarnowski W., Just K., *Model of the Electromagnetic Linear Actuator for Optimization Purposes*, 23rd European Conference on Modelling and Simulation (ECMS), Madrid, SPAIN, 2009, pp. 708-714.

K. JUST, P. PISKUR

**Badanie wpływu kierunku magnesowania na własności statyczne i dynamiczne liniowego przetwornika elektromechanicznego**

**Streszczenie.** W artykule przedstawiono analizę wpływu kierunku magnesowania magnesów trwałych na charakterystyki statyczne oraz dynamiczne liniowego przetwornika elektromechanicznego. Obliczenia symulacyjne przeprowadzono dla trzech różnych konfiguracji kierunku magnesowania magnesów trwałych (osiowej, promieniowej oraz tzw. tablicy Halbacha). W obliczeniach wykorzystano metodę elementów skończonych (MES), której zastosowanie zapewnia dobre odwzorowanie własności rzeczywistego obiektu. Przeprowadzone obliczenia pozwoliły na zbadanie i ocenę wpływu kierunku magnetyzacji biegnika na własności statyczne oraz dynamiczne napędu.

**Słowa kluczowe:** modelowanie i symulacja, napęd elektromagnetyczny, metoda elementów skończonych, analiza pola elektromagnetycznego, tablica Halbacha

**DOI:** 10.5604/01.3001.0012.0956